Chapter 6
Longitudinal Dynamics

6.1 RESPONSE TO CONTROLS

The solution of the longitudinal equations of motion by, for example, the methods described in Chapter 5 enables the response transfer functions to be obtained. These completely describe the linear dynamic response to a control input in the plane of symmetry. Implicit in the response are the dynamic properties determined by the stability characteristics of the aeroplane. The transfer functions and the response variables described by them are linear since the entire modelling process is based on the assumption that the motion is constrained to small disturbances about an equilibrium trim state. However, it is common practice to assume that the response to controls is valid when the magnitude of the response can hardly be described as "a small perturbation". For many conventional aeroplanes the error incurred by so doing is generally acceptably small as such aeroplanes tend to have substantially linear aerodynamic characteristics over their flight envelopes. For aeroplanes with very large flight envelopes, significant aerodynamic non-linearity and, or, dependence on sophisticated flight control systems, it is advisable not to use the linearised equations of motion for analysis of response other than that which can justifiably be described as being of small magnitude.

It is convenient to review the longitudinal response to elevator about a trim state in which the thrust is held constant. The longitudinal state equation (4.67) may then be written:

$$\begin{bmatrix} \dot{u} \\ \dot{w} \\ \dot{q} \\ \dot{\theta} \end{bmatrix} = \begin{bmatrix} x_u & x_w & x_q & x_\theta \\ z_u & z_w & z_q & z_\theta \\ m_u & m_w & m_q & m_\theta \\ 0 & 0 & 1 & 0 \end{bmatrix} \begin{bmatrix} u \\ w \\ q \\ \theta \end{bmatrix} + \begin{bmatrix} x_\eta \\ z_\eta \\ m_\eta \\ 0 \end{bmatrix} \eta \tag{6.1}$$

The four response transfer functions obtained in the solution of equation (6.1) may conveniently be written:

$$\frac{u(s)}{\eta(s)} \equiv \frac{N_\eta^u(s)}{\Delta(s)} = \frac{k_u(s + 1/T_u)(s^2 + 2\zeta_u\omega_u s + \omega_u^2)}{(s^2 + 2\zeta_p\omega_p s + \omega_p^2)(s^2 + 2\zeta_s\omega_s s + \omega_s^2)} \tag{6.2}$$

$$\frac{w(s)}{\eta(s)} \equiv \frac{N_\eta^w(s)}{\Delta(s)} = \frac{k_w(s + 1/T_\alpha)(s^2 + 2\zeta_\alpha\omega_\alpha s + \omega_\alpha^2)}{(s^2 + 2\zeta_p\omega_p s + \omega_p^2)(s^2 + 2\zeta_s\omega_s s + \omega_s^2)} \tag{6.3}$$

$$\frac{q(s)}{\eta(s)} \equiv \frac{N_\eta^q(s)}{\Delta(s)} = \frac{k_q s(s+(1/T_{\theta_1}))(s+(1/T_{\theta_2}))}{(s^2+2\zeta_p\omega_p s+\omega_p^2)(s^2+2\zeta_s\omega_s s+\omega_s^2)} \tag{6.4}$$

$$\frac{\theta(s)}{\eta(s)} \equiv \frac{N_\eta^\theta(s)}{\Delta(s)} = \frac{k_\theta(s+(1/T_{\theta_1}))(s+(1/T_{\theta_2}))}{(s^2+2\zeta_p\omega_p s+\omega_p^2)(s^2+2\zeta_s\omega_s s+\omega_s^2)} \tag{6.5}$$

The solution of the equations of motion results in polynomial descriptions of the transfer function numerators and common denominator as set out in Appendix 3. The polynomials factorise into real and complex pairs of roots that are most explicitly quoted in the style of equations (6.2)–(6.5) above. Since the roots are interpreted as time constants, damping ratios and natural frequencies the above style of writing makes the essential information instantly available. It should also be noted that the numerator and denominator factors are typical for a conventional aeroplane. Sometimes complex pairs of roots may become two real roots and *vice versa*. However, this does not usually mean that the dynamic response characteristics of the aeroplane become dramatically different. Differences in the interpretation of response may be evident but will not necessarily be large.

As has already been indicated, the common denominator of the transfer functions describes the characteristic polynomial which, in turn, describes the stability characteristics of the aeroplane. Thus the response of all variables to an elevator input is dominated by the denominator parameters namely, damping ratios and natural frequencies. The differences between the individual responses is entirely determined by their respective numerators. It is therefore important to fully appreciate the role of the numerator in determining response dynamics. The *response shapes* of the individual variables are determined by the common denominator and "coloured" by their respective numerators. The numerator plays no part in determining stability in a linear system which is how the aeroplane is modelled here.

Example 6.1

The equations of motion and aerodynamic data for the Ling-Temco-Vought A-7A Corsair II aircraft were obtained from Teper (1969). The flight condition corresponds to level cruising flight at an altitude of 15,000 ft at Mach 0.3. The equations of motion, referred to a body axis system, arranged in state space format are

$$\begin{bmatrix} \dot{u} \\ \dot{w} \\ \dot{q} \\ \dot{\theta} \end{bmatrix} = \begin{bmatrix} 0.00501 & 0.00464 & -72.90000 & -31.34000 \\ -0.08570 & -0.54500 & 309.00000 & -7.40000 \\ 0.00185 & -0.00767 & -0.39500 & 0.00132 \\ 0 & 0 & 1 & 0 \end{bmatrix} \begin{bmatrix} u \\ w \\ q \\ \theta \end{bmatrix} + \begin{bmatrix} 5.63000 \\ -23.80000 \\ -4.51576 \\ 0 \end{bmatrix} \eta \tag{6.6}$$

Since incidence α and flight path angle γ are useful variables in the evaluation of handling qualities, it is convenient to augment the corresponding output equation, as

described in paragraph 5.7, in order to obtain their response transfer functions in the solution of the equations of motion. The output equation is therefore,

$$\begin{bmatrix} u \\ w \\ q \\ \theta \\ \alpha \\ \gamma \end{bmatrix} = \begin{bmatrix} 1 & 0 & 0 & 0 \\ 0 & 1 & 0 & 0 \\ 0 & 0 & 1 & 0 \\ 0 & 0 & 0 & 1 \\ 0 & 0.00316 & 0 & 0 \\ 0 & -0.00316 & 0 & 1 \end{bmatrix} \begin{bmatrix} u \\ w \\ q \\ \theta \end{bmatrix} + \begin{bmatrix} 0 \\ 0 \\ 0 \\ 0 \\ 0 \\ 0 \end{bmatrix} \eta \tag{6.7}$$

Note that all elements in the matrices in equations (6.6) and (6.7) have been rounded to five decimal places simply to keep the equations to a reasonable physical size. This should not be done with the equations used in the actual computation.

Solution of the equations of motion using *Program CC* determines the following response transfer functions:

$$\begin{aligned}
\frac{u(s)}{\eta(s)} &= \frac{5.63(s+0.369)(s+0.587)(s+58.437)}{(s^2+0.033s+0.020)(s^2+0.902s+2.666)} \text{ ft/s/rad} \\
\frac{w(s)}{\eta(s)} &= \frac{-23.8(s^2-0.0088s+0.0098)(s+59.048)}{(s^2+0.033s+0.020)(s^2+0.902s+2.666)} \text{ ft/s/rad} \\
\frac{q(s)}{\eta(s)} &= \frac{-4.516s(s-0.008)(s+0.506)}{(s^2+0.033s+0.020)(s^2+0.902s+2.666)} \text{ rad/s/rad (deg/s/deg)} \\
\frac{\theta(s)}{\eta(s)} &= \frac{-4.516(s-0.008)(s+0.506)}{(s^2+0.033s+0.020)(s^2+0.902s+2.666)} \text{ rad/rad (deg/deg)} \\
\frac{\alpha(s)}{\eta(s)} &= \frac{-0.075(s^2-0.0088s+0.0098)(s+59.048)}{(s^2+0.033s+0.020)(s^2+0.902s+2.666)} \text{ rad/rad (deg/deg)} \\
\frac{\gamma(s)}{\eta(s)} &= \frac{0.075(s-0.027)(s+5.004)(s-6.084)}{(s^2+0.033s+0.020)(s^2+0.902s+2.666)} \text{ rad/rad (deg/deg)}
\end{aligned} \tag{6.8}$$

All coefficients have again been rounded to a convenient number of decimal places and the above caution should be noted.

The characteristic equation is given by equating the common denominator polynomial to zero:

$$\Delta(s) = (s^2+0.033s+0.020)(s^2+0.902s+2.666) = 0$$

The first pair of complex roots describes the phugoid stability mode, with characteristics:

Damping ratio	$\zeta_p = 0.11$
Undamped natural frequency	$\omega_p = 0.14$ rad/s

The second pair of complex roots describes the short period pitching oscillation, or short period stability mode, with characteristics:

Damping ratio	$\zeta_s = 0.28$
Undamped natural frequency	$\omega_s = 1.63$ rad/s

These mode characteristics indicate that the airframe is aerodynamically stable although it will be shown later that the short-period mode damping ratio is unacceptably low.

The response of the aircraft to a unit step (1°) elevator input is shown in Fig. 6.1. All of the variables in the solution of the equations of motion are shown the responses being characterised by the transfer functions, equations (6.8).

The responses clearly show both dynamic stability modes, the short period pitching oscillation and the phugoid. However, the magnitude of each stability mode differs in each response variable. For example, the short period pitching oscillation is most visible as the initial transient in the variables w, q and α whereas the phugoid mode is visible in all variables although the relative magnitudes vary considerably. Clearly the stability of the responses is the same, as determined by the common denominator of the transfer functions, equations (6.8), but the differences between each of the response variables is determined by the unique numerator of each response transfer function.

The mode content in each of the motion variables is given most precisely by the eigenvectors. The analytical procedure described in Example 5.7 is applied to the equations of motion for the A-7A. With the aid of *MATLAB* the eigenvector matrix **V** is determined as follows:

$$\mathbf{V} = \begin{array}{c} \begin{matrix} \text{Short period mode} & & \text{Phugoid mode} & \end{matrix} \\ \left[\begin{array}{cc|cc} -0.1682 - 0.1302j & -0.1682 + 0.1302j & 0.1467 + 0.9677j & 0.1467 - 0.9677j \\ 0.2993 + 0.9301j & 0.2993 - 0.9301j & 0.0410 + 0.2008j & 0.0410 - 0.2008j \\ -0.0046 + 0.0018j & -0.0046 - 0.0018j & 0.0001 + 0.0006j & 0.0001 - 0.0006j \\ 0.0019 + 0.0024j & 0.0019 - 0.0024j & 0.0041 - 0.0013j & 0.0041 + 0.0013j \end{array}\right] \begin{array}{l} : u \\ : w \\ : q \\ : \theta \end{array} \end{array} \tag{6.9}$$

To facilitate interpretation of the eigenvector matrix, the magnitude of each component eigenvector is calculated as follows:

$$\left[\begin{array}{cc|cc} 0.213 & 0.213 & 0.979 & 0.979 \\ 0.977 & 0.977 & 0.204 & 0.204 \\ 0.0049 & 0.0049 & 0.0006 & 0.0006 \\ 0.0036 & 0.0036 & 0.0043 & 0.0043 \end{array}\right] \begin{array}{l} : u \\ : w \\ : q \\ : \theta \end{array}$$

Clearly, the phugoid mode is dominant in u since $0.979 \gg 0.213$, the short period mode is dominant in w since $0.977 \gg 0.204$, the short period mode is dominant in q since $0.0049 \gg 0.0006$ and the short period and phugoid modes content in θ are of a similar order. These observations accord very well with the responses shown in Fig. 6.1.

The steady state values of the variables following a unit step (1°) elevator input may be determined by application of the final value theorem, equation (5.33). The

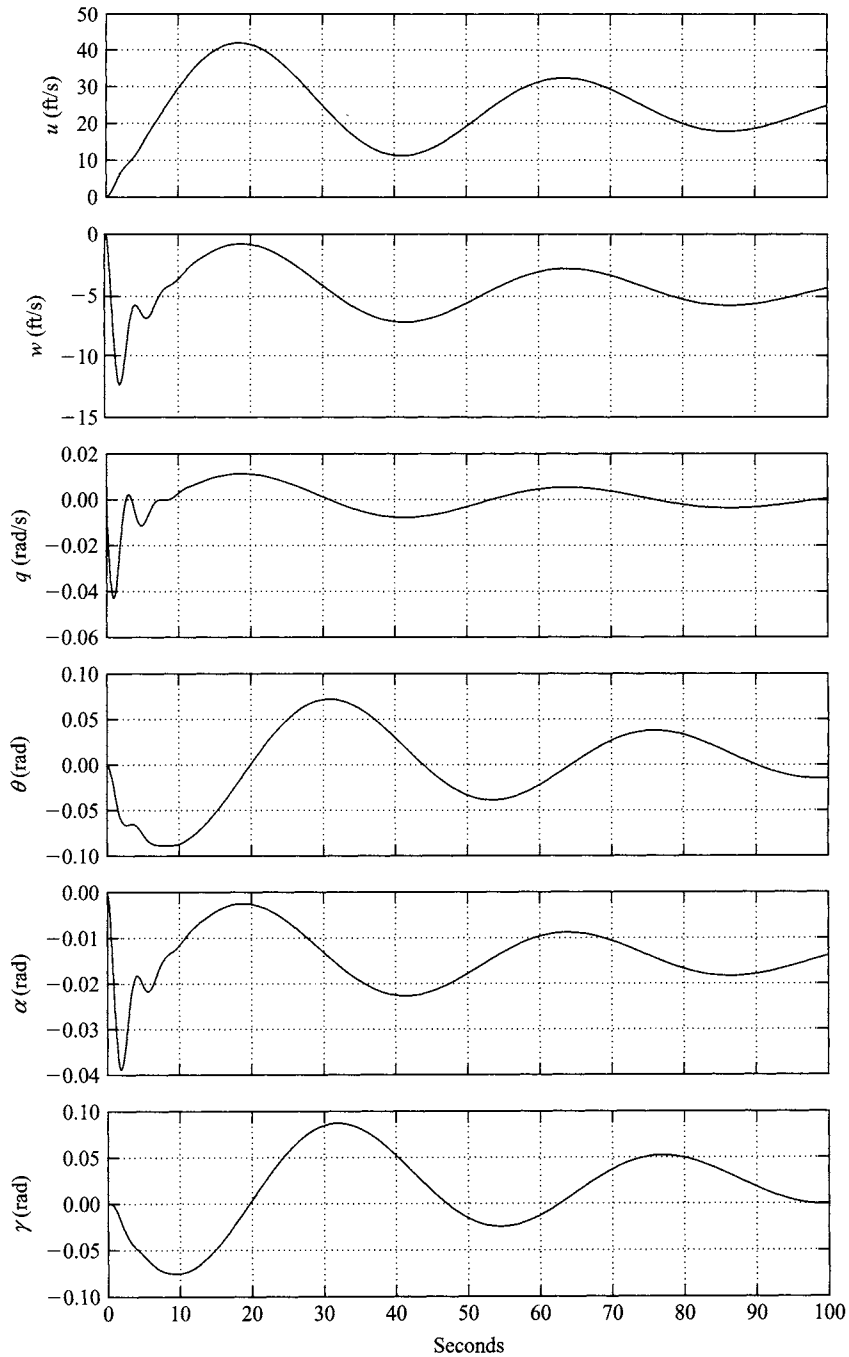

Figure 6.1 *Aircraft response to 1° elevator step input.*

transfer functions, equations (6.8), assume a unit elevator displacement to mean 1 rad and this has transfer function:

$$\eta(s) = \frac{1}{s} \text{ rad}$$

For a unit step input of 1° the transfer function becomes

$$\eta(s) = \frac{1}{57.3s} = \frac{0.0175}{s} \text{ rad}$$

Thus, for example, the Laplace transform of the speed response to a 1° elevator step input is given by

$$u(s) = \frac{5.63(s + 0.369)(s + 0.587)(s + 58.437)}{(s^2 + 0.033s + 0.020)(s^2 + 0.902s + 2.666)} \frac{0.0175}{s} \text{ ft/s}$$

Applying the final value theorem, equation (5.33):

$$\begin{aligned} u(t)|_{ss} &= \operatorname*{Lim}_{s \to 0} \left(s \frac{5.63(s + 0.369)(s + 0.587)(s + 58.437)}{(s^2 + 0.033s + 0.020)(s^2 + 0.902s + 2.666)} \frac{0.0175}{s} \right) \text{ ft/s} \\ &= 23.39 \text{ ft/s} \end{aligned}$$

Since the step input is positive in the nose down sense the response eventually settles to the small steady increase in speed indicated.

In a similar way the steady state response of all the motion variables may be calculated to give

$$\begin{bmatrix} u \\ w \\ q \\ \theta \\ \alpha \\ \gamma \end{bmatrix}_{\substack{\text{steady} \\ \text{state}}} = \begin{bmatrix} 23.39 \text{ ft/s} \\ -4.53 \text{ ft/s} \\ 0 \\ 0.34° \\ -0.81° \\ 1.15° \end{bmatrix} \tag{6.10}$$

It is important to remember that the steady state values given in equation (6.10) represent the *changes* with respect to the initial equilibrium trim state following the 1° elevator step input. Although the initial response is applied in the nose down sense, inspection of equation (6.10) indicates that after the mode transients have damped out the aircraft is left with a small reduction in incidence, a small increase in pitch attitude and is climbing steadily at a flight path angle of 1.15°. This apparent anomaly is due to the fact that at the chosen flight condition the aircraft is operating close to the stall boundary on the *back side* of the drag-speed curve, that is, below the minimum drag speed. Thus the disturbance results in a significant decrease in drag leaving the aircraft with sufficient excess power enabling it to climb gently. It is for the same reason that a number of the transfer functions (6.8), have non-minimum phase numerator terms where these would not normally be expected.

6.1.1 The characteristic equation

The longitudinal characteristic polynomial for a classical aeroplane is fourth order; it determines the common denominator in the longitudinal response transfer functions and, when equated to zero, defines the characteristic equation which may be written:

$$As^4 + Bs^3 + Cs^2 + Ds + E = 0 \tag{6.11}$$

The characteristic equation (6.11) most commonly factorises into two pairs of complex roots which are most conveniently written:

$$(s^2 + 2\zeta_p\omega_p s + \omega_p^2)(s^2 + 2\zeta_s\omega_s s + \omega_s^2) = 0 \tag{6.12}$$

As already explained, the second order characteristics in equation (6.12) describe the phugoid and short period stability modes respectively. The stability modes comprising equation (6.12) provide a *complete description* of the longitudinal stability properties of the aeroplane subject to the constraint of small perturbation motion. Interpretation of the characteristic equation written in this way is most readily accomplished if reference is first made to the properties of the classical mechanical mass-spring-damper system which are summarised in Appendix 6.

Thus the longitudinal dynamics of the aeroplane may be likened to a pair of loosely coupled mass-spring-damper systems and the interpretation of the motion of the aeroplane following a disturbance from equilibrium may be made by direct comparison with the behaviour of the mechanical mass-spring-damper. However, the damping and frequency characteristics of the aeroplane are obviously not mechanical in origin, they derive entirely from the aerodynamic properties of the airframe. The connection between the observed dynamics of the aeroplane and its aerodynamic characteristics is made by comparing equation (6.12) with equation (6.11) and then referring to Appendix 3 for the definitions of the coefficients in equation (6.11) in terms of aerodynamic stability derivatives. Clearly, the relationships between the damping ratios and undamped frequencies of equation (6.12) and their aerodynamic *drivers* are neither obvious nor simple. Means for dealing with this difficulty are described below in which simplifying approximations are made based on the observation and understanding of the physical behaviour of aeroplane dynamics.

6.2 THE DYNAMIC STABILITY MODES

Both longitudinal dynamic stability modes are excited whenever the aeroplane is disturbed from its equilibrium trim state. A disturbance may be initiated by pilot control inputs, a change in power setting, airframe configuration changes such as flap deployment and by external atmospheric influences such as gusts and turbulence.

6.2.1 The short period pitching oscillation

The short period mode is typically a damped oscillation in pitch about the *oy* axis. Whenever an aircraft is disturbed from its pitch equilibrium state the mode is excited

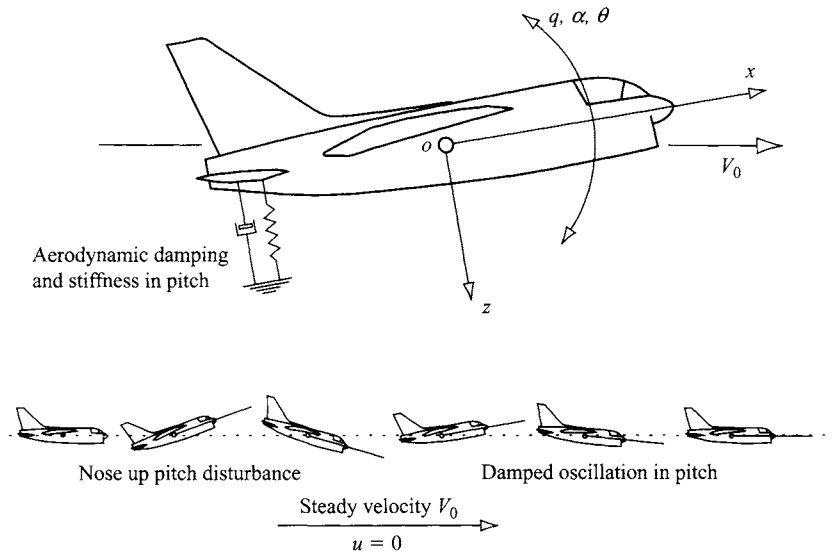

Figure 6.2 *A stable short period pitching oscillation.*

and manifests itself as a classical second order oscillation in which the principal variables are incidence $\alpha(w)$, pitch rate q and pitch attitude θ. This observation is easily confirmed by reference to the eigenvectors in the solution of the equations of motion; this may be seen in Example 6.1 and also in Fig. 6.1. Typically the undamped natural frequency of the mode is in the range 1 rad/s to 10 rad/s and the damping is usually stabilising although the damping ratio is often lower than desired. A significant feature of the mode is that the speed remains approximately constant ($u = 0$) during a disturbance. As the period of the mode is short, inertia and momentum effects ensure that speed response in the time scale of the mode is negligible.

The physical situation applying can be interpreted by comparison with a torsional mass-spring-damper system. The aircraft behaves as if it were restrained by a torsional spring about the *oy* axis as indicated in Fig. 6.2. A pitch disturbance from trim equilibrium causes the "spring" to produce a restoring moment thereby giving rise to an oscillation in pitch. The oscillation is damped and this can be interpreted as a viscous damper as suggested in Fig. 6.2. Of course the spring and viscous damping effects are not mechanical. In reality they are produced entirely by aerodynamic mechanisms with contributions from all parts of the airframe, not all of which are necessarily stabilising in effect. However, in the interests of promoting understanding, the stiffness and damping effects are assumed to be dominated by the aerodynamics of the tailplane. The spring stiffness arises from the natural *weathercock* tendency of the tailplane to align with the incident flow. The damping arises from the motion of the tailplane during the oscillation when, clearly, it behaves as a kind of viscous paddle damper. The total observed mode dynamics depend not only on the tailplane contribution, but also on the magnitudes of the additional contributions from other parts of the airframe. When the overall stability is marginal it is implied that the additional contributions are also significant and it becomes much more difficult to identify and quantify the principal aerodynamic mode drivers.

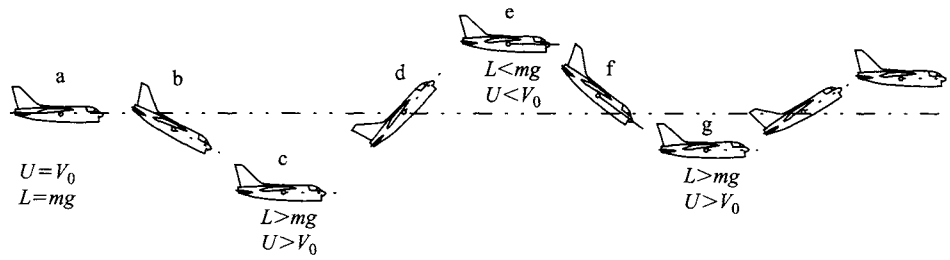

Figure 6.3 *The development of a stable phugoid.*

6.2.2 The phugoid

The phugoid mode is most commonly a lightly damped low frequency oscillation in speed u which couples into pitch attitude θ and height h. A significant feature of this mode is that the incidence $\alpha(w)$ remains substantially constant during a disturbance. Again, these observations are easily confirmed by reference to the eigenvectors in the solution of the equations of motion, this may be seen in Example 6.1 and also in Fig. 6.1. However, it is clear that the phugoid appears, to a greater or lesser extent, in all of the longitudinal motion variables but the relative magnitudes of the phugoid components in incidence $\alpha(w)$ and in pitch rate q are very small. Typically, the undamped natural frequency of the phugoid is in the range 0.1 rad/s to 1 rad/s and the damping ratio is very low. However, the apparent damping characteristics of the mode may be substantially influenced by power effects in some aeroplanes.

Consider the development of classical phugoid motion following a small disturbance in speed as shown in Fig. 6.3. Initially the aeroplane is in trimmed level equilibrium flight with steady velocity V_0 such that the lift L and weight mg are equal. Let the aeroplane be disturbed at (a) such that the velocity is reduced by a small amount u. Since the incidence remains substantially constant this results in a small reduction in lift such that the aeroplane is no longer in vertical equilibrium. It therefore starts to lose height and since it is flying "down hill" it starts to accelerate as at (b). The speed continues to build up to a value in excess of V_0 which is accompanied by a build up in lift which eventually exceeds the weight by a significant margin. The build up in speed and lift cause the aircraft to pitch up steadily until at (c) it starts to climb. Since it now has an excess of kinetic energy, inertia and momentum effects cause it to fly up through the nominal trimmed height datum at (d) losing speed and lift as it goes as it is now flying "up hill". As it decelerates it pitches down steadily until at (e) its lift is significantly less than the weight and the accelerating descent starts again. Inertia and momentum effects cause the aeroplane to continue flying down through the nominal trimmed height datum (f) and as the speed and lift continue to build up so it pitches up steadily until at (g) it starts climbing again to commence the next cycle of oscillation. As the motion progresses the effects of drag cause the motion variable maxima and minima at each peak to reduce gradually in magnitude until the motion eventually damps out.

Thus the phugoid is classical damped harmonic motion resulting in the aircraft flying a gentle sinusoidal flight path about the nominal trimmed height datum. As large inertia and momentum effects are involved the motion is necessarily relatively

slow such that the angular accelerations, $\dot{q}$ and $\dot{\alpha}(\dot{w})$, are insignificantly small. Consequently, the natural frequency of the mode is low and since drag is designed to be low so the damping is also low. Typically, once excited many cycles of the phugoid may be visible before it eventually damps out. Since the rate of loss of energy is low, a consequence of low drag damping effects, the motion is often approximated by undamped harmonic motion in which potential and kinetic energy are exchanged as the aircraft flies the sinusoidal flight path. This in fact was the basis on which Lanchester (1908) first successfully analysed the motion.

6.3 REDUCED ORDER MODELS

Thus far the emphasis has been on the exact solution of the longitudinal equations of motion which results in an exact description of the stability and response characteristics of the aircraft. Although this is usually the object of a flight dynamics investigation it has two disadvantages. First, a computational facility is required if a very tedious manual solution is to be avoided and, second, it is difficult, if not impossible, to establish the relationships between the stability characteristics and their aerodynamic drivers. Both these disadvantages can be avoided by seeking approximate solutions that can also provide considerable insight into the physical phenomena governing the dynamic behaviour of the aircraft.

For example, an approximate solution of the longitudinal characteristic equation (6.11) is based on the fact that the coefficients A, B, C, D and E have relative values that do not change very much for conventional aeroplanes. Generally A, B and C are significantly larger than D and E such that the quartic has the following approximate factors:

$$A\left(s^2 + \frac{(CD - BE)}{C^2}s + \frac{E}{C}\right)\left(s^2 + \frac{B}{A}s + \frac{C}{A}\right) = 0 \tag{6.13}$$

Equation (6.13) is in fact the first step in the classical manual iterative solution of the quartic; the first pair of complex roots describes the phugoid and the second pair describes the short period mode. Algebraic expressions, in terms of aerodynamic derivatives, mass and inertia parameters, etc., for the coefficients A, B, C, D and E are given in Appendix 3. As these expressions are relatively complex further physical insight is not particularly revealing unless simplifying assumptions are made. However, the approximate solution given by equation (6.13) is often useful for preliminary mode evaluations, or as a check of computer solutions, when the numerical values of the coefficients A, B, C, D and E are known. For conventional aeroplanes the approximate solution is often surprisingly close to the exact solution of the characteristic equation.

6.3.1 The short period mode approximation

The short term response characteristics of an aircraft are of particular importance in flying and handling qualities considerations for the reasons stated in Section 6.5. Since

short term behaviour is dominated by the short period mode it is convenient to obtain the *reduced-order* equations of motion in which the phugoid is suppressed or omitted. By observing the nature of the short period pitching oscillation, sometimes called the *rapid incidence adjustment*, it is possible to simplify the longitudinal equations of motion to describe short term dynamics only. The terms remaining in the reduced-order equations of motion are therefore the terms that dominate short term dynamics thereby providing insight into the important aerodynamic drivers governing physical behaviour.

It has already been established that the short period pitching oscillation is almost exclusively an oscillation in which the principal variables are pitch rate q and incidence α, the speed remaining essentially constant, thus $u = 0$. Therefore, the speed equation and the speed dependent terms may be removed from the longitudinal equations of motion 6.1; since they are all approximately zero in short term motion, the revised equations may be written:

$$\begin{bmatrix} \dot{w} \\ \dot{q} \\ \dot{\theta} \end{bmatrix} = \begin{bmatrix} z_w & z_q & z_\theta \\ m_w & m_q & m_\theta \\ 0 & 1 & 0 \end{bmatrix} \begin{bmatrix} w \\ q \\ \theta \end{bmatrix} + \begin{bmatrix} z_\eta \\ m_\eta \\ 0 \end{bmatrix} \eta \tag{6.14}$$

Further, assuming the equations of motion are referred to aircraft wind axes and that the aircraft is initially in steady level flight then

$$\theta_e \equiv \alpha_e = 0 \quad \text{and} \quad U_e = V_0$$

and, with reference to Appendix 2, it follows that

$$z_\theta = m_\theta = 0$$

Equation (6.14) then reduces to its simplest possible form:

$$\begin{bmatrix} \dot{w} \\ \dot{q} \end{bmatrix} = \begin{bmatrix} z_w & z_q \\ m_w & m_q \end{bmatrix} \begin{bmatrix} w \\ q \end{bmatrix} + \begin{bmatrix} z_\eta \\ m_\eta \end{bmatrix} \eta \tag{6.15}$$

where now, the derivatives are referred to a wind axes system. Equation (6.15) is sufficiently simple that the transfer function matrix may be calculated manually by the application of equation (5.53):

$$\mathbf{G}(s) = \frac{\mathbf{N}(s)}{\Delta(s)} = \frac{\begin{bmatrix} s - m_q & z_q \\ m_w & s - z_w \end{bmatrix} \begin{bmatrix} z_\eta \\ m_\eta \end{bmatrix}}{\begin{vmatrix} s - z_w & -z_q \\ -m_w & s - m_q \end{vmatrix}}$$

$$= \frac{\begin{bmatrix} z_\eta \left(s + \left(m_q + z_q \dfrac{m_\eta}{z_\eta} \right) \right) \\ m_\eta \left(s + \left(m_w \dfrac{z_\eta}{m_\eta} - z_w \right) \right) \end{bmatrix}}{(s^2 - (m_q + z_w)s + (m_q z_w - m_w z_q))} \tag{6.16}$$

The transfer functions may be further simplified by noting that

$$z_q \frac{m_\eta}{z_\eta} \gg m_q \quad \text{and} \quad -z_w \gg m_w \frac{z_\eta}{m_\eta}$$

and with reference to Appendix 2:

$$z_q = \frac{\overset{\circ}{Z}_q + mU_e}{m - \overset{\circ}{Z}_{\dot{w}}} \cong U_e$$

since

$$\overset{\circ}{Z}_q \ll mU_e \quad \text{and} \quad m \gg \overset{\circ}{Z}_{\dot{w}}$$

Thus the two short term transfer functions describing response to elevator may be written:

$$\frac{w(s)}{\eta(s)} = \frac{z_\eta \left(s + U_e \frac{m_\eta}{z_\eta}\right)}{(s^2 - (m_q + z_w)s + (m_q z_w - m_w U_e))} \equiv \frac{k_w(s + 1/T_\alpha)}{(s^2 + 2\zeta_s \omega_s s + \omega_s^2)} \tag{6.17}$$

$$\frac{q(s)}{\eta(s)} = \frac{m_\eta(s - z_w)}{(s^2 - (m_q + z_w)s + (m_q z_w - m_w U_e))} \equiv \frac{k_q(s + 1/T_{\theta_2})}{(s^2 + 2\zeta_s \omega_s s + \omega_s^2)} \tag{6.18}$$

where now it is understood that k_w, k_q, T_α, T_{θ_2}, ζ_s and ω_s represent approximate values. Clearly it is now very much easier to relate the most important parameters describing longitudinal short term transient dynamics of the aircraft to the aerodynamic properties of the airframe, represented in equations (6.17) and (6.18) by the concise derivatives.

The reduced order characteristic equation may be written down on inspection of equation (6.17) or (6.18):

$$\Delta(s) = s^2 + 2\zeta_s \omega_s s + \omega_s^2 = s^2 - (m_q + z_w)s + (m_q z_w - m_w U_e) = 0 \tag{6.19}$$

and, by analogy with the classical mass-spring-damper system described in Appendix 6, the damping and natural frequency of the short period mode are given, to a good approximation, by

$$\begin{aligned} 2\zeta_s \omega_s &= -(m_q + z_w) \\ \omega_s &= \sqrt{m_q z_w - m_w U_e} \end{aligned} \tag{6.20}$$

It is instructive to write the damping and natural frequency expressions (6.20) in terms of the dimensional derivatives. The appropriate conversions are obtained from

Appendix 2 and the assumptions made above are applied to give

$$2\zeta_s\omega_s = -\left(\frac{\overset{\circ}{M}_q}{I_y} + \frac{\overset{\circ}{Z}_w}{m} + \frac{\overset{\circ}{M}_{\dot{w}}U_e}{I_y}\right)$$

$$\omega_s = \sqrt{\frac{\overset{\circ}{M}_q}{I_y}\frac{\overset{\circ}{Z}_w}{m} - \frac{\overset{\circ}{M}_w U_e}{I_y}} \tag{6.21}$$

Note that the terms on the right hand side of expressions (6.21) comprise aerodynamic derivatives divided either by mass or moment of inertia in pitch. These terms may be interpreted in exactly the same way as those of the classical mass-spring-damper. Thus, it becomes apparent that the aerodynamic derivatives are providing stiffness and viscous damping in pitch although there is more than one term contributing to damping and to natural frequency. Therefore the aerodynamic origins of the short period dynamics are a little more complex than those of the classical mass-spring-damper and the various contributions do not always act in the most advantageous way. However, for conventional aeroplanes the overall dynamic characteristics usually describe a stable short period mode.

For a typical conventional aeroplane the relative magnitudes of the aerodynamic derivatives are such that to a crude approximation:

$$2\zeta_s\omega_s = \frac{-\overset{\circ}{M}_q}{I_y}$$

$$\omega_s = \sqrt{\frac{-\overset{\circ}{M}_w U_e}{I_y}} \tag{6.22}$$

which serves only to indicate what are usually regarded as the dominant terms governing the short period mode. Normally the derivative $\overset{\circ}{Z}_w$, which is dependent on the lift curve slope of the wing, and the derivative $\overset{\circ}{M}_q$, which is determined largely by the viscous "paddle" damping properties of the tailplane, are both negative numbers. The derivative $\overset{\circ}{M}_w$ is a measure of the aerodynamic stiffness in pitch and is also dominated by the aerodynamics of the tailplane. The sign of $\overset{\circ}{M}_w$ depends on the position of the *cg*, becoming increasingly negative as the *cg* moves forward in the airframe. Thus the short period mode will be stable if the *cg* is far enough forward in the airframe. The *cg* position in the airframe where $\overset{\circ}{M}_w$ changes sign is called the *controls fixed neutral point* and $\overset{\circ}{M}_w$ is therefore also a measure of the *controls fixed stability margin* of the aircraft. With reference to equation (6.19) and expressions (6.20), the corresponding *cg* position where $(m_q z_w - m_w U_e)$ changes sign is called the *controls fixed manoeuvre point* and $(m_q z_w - m_w U_e)$ is a measure of the *controls fixed manoeuvre margin* of the aircraft. The subject of manoeuvrability is discussed in Chapter 8.

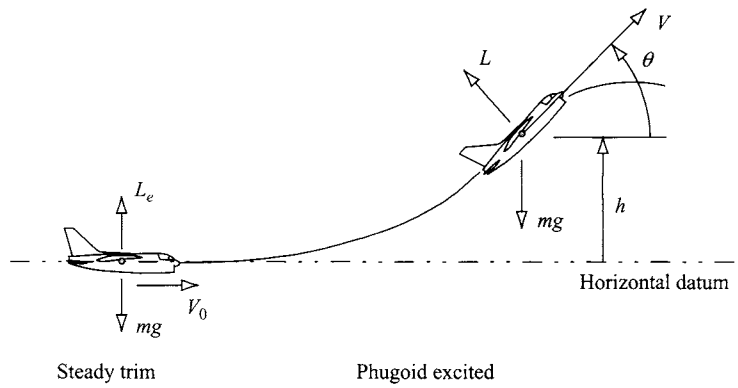

Figure 6.4 *The phugoid oscillation.*

6.3.2 The phugoid mode approximation

A reduced order model of the aircraft retaining only the phugoid dynamics is very rarely required in flight dynamics studies. However, the greatest usefulness of such a model is to identify those aerodynamic properties of the airframe governing the characteristics of the mode.

6.3.2.1 The Lanchester model

Probably the first successful analysis of aeroplane dynamics was made by Lanchester (1908) who devised a mathematical model to describe phugoid motion based on his observations of the behaviour of gliding model aeroplanes. His analysis gives excellent insight into the physical nature of the mode and may be applied to the modern aeroplane by interpreting and restating his original assumptions as follows:

(i) The aircraft is initially in steady level flight.
(ii) The total energy of the aircraft remains constant.
(iii) The incidence α remains constant at its initial trim value.
(iv) The thrust τ balances the drag D.
(v) The motion is sufficiently slow that pitch rate q effects may be ignored.

Referring to Fig. 6.4 the aircraft is initially in trimmed straight level flight with velocity V_0. Following a disturbance in speed which excites the phugoid mode the disturbed speed, pitch attitude and height are denoted V, θ and h respectively. Then based on assumption (ii):

$$\frac{1}{2}mV_0^2 = \frac{1}{2}mV^2 + mgh = \text{constant}$$

whence

$$V^2 = V_0^2 - 2gh \tag{6.23}$$

which describes the exchange of kinetic and potential energy as the aeroplane flies the sinusoidal flight path.

In the initial steady trim state the lift and weight are in balance thus

$$L_e = \frac{1}{2}\rho V_0^2 S C_L = mg \tag{6.24}$$

and in disturbed flight the lift is given by

$$L = \frac{1}{2}\rho V^2 S C_L \tag{6.25}$$

As a consequence of assumption (iii) the lift coefficient C_L also remains constant and equations (6.23)–(6.25) may be combined to give

$$L = mg - \rho g h S C_L \tag{6.26}$$

Since simple undamped oscillatory motion is assumed, a consequence of assumption (ii), the single degree of freedom equation of motion in height may be written:

$$m\ddot{h} = L\cos\theta - mg \cong L - mg \tag{6.27}$$

since, by definition, θ is a small angle. Substituting for lift L from equation (6.26) into equation (6.27):

$$\ddot{h} + \left(\frac{\rho g S C_L}{m}\right) h = \ddot{h} + \omega_p^2 h = 0 \tag{6.28}$$

Thus, approximately, the frequency of the phugoid mode is given by

$$\omega_p = \sqrt{\frac{\rho g S C_L}{m}} = \frac{g\sqrt{2}}{V_0} \tag{6.29}$$

when equation (6.24) is used to eliminate the mass.

Thus, to a reasonable approximation, Lanchester's model shows that the phugoid frequency is inversely proportional to the steady trimmed speed about which the mode oscillates and that its damping is zero.

6.3.2.2 *A reduced order model*

A more detailed approximate model of the phugoid mode may be derived from the equations of motion by making simplifications based on assumptions about the nature of the motion. Following a disturbance, the variables $w(\alpha)$ and q respond in the time scale associated with the short period mode; thus, it is reasonable to assume that $w(\alpha)$ and q are quasi-steady in the longer time scale associated with the phugoid. Whence, it follows that

$$\dot{w} = \dot{q} = 0$$

Once again, it is assumed that the equations of motion are referred to aircraft wind axes and since the disturbance takes place about steady level flight then

$$\theta_e \equiv \alpha_e = 0 \quad \text{and} \quad U_e = V_0$$

and, with reference to Appendix 2, it follows that

$$x_\theta = -g \quad \text{and} \quad z_\theta = m_\theta = 0$$

Also, as for the reduced order short period model and with reference to Appendix 2:

$$z_q = \frac{\overset{\circ}{Z}_q + mU_e}{m - \overset{\circ}{Z}_{\dot{w}}} \cong U_e$$

since

$$\overset{\circ}{Z}_q \ll mU_e \quad \text{and} \quad m \gg \overset{\circ}{Z}_{\dot{w}}$$

Additionally, it is usually assumed that the aerodynamic derivative x_q is insignificantly small. Thus the equations of motion (6.1) may be simplified accordingly:

$$\begin{bmatrix} \dot{u} \\ 0 \\ 0 \\ \dot{\theta} \end{bmatrix} = \begin{bmatrix} x_u & x_w & 0 & -g \\ z_u & z_w & U_e & 0 \\ m_u & m_w & m_q & 0 \\ 0 & 0 & 1 & 0 \end{bmatrix} \begin{bmatrix} u \\ w \\ q \\ \theta \end{bmatrix} + \begin{bmatrix} x_\eta \\ z_\eta \\ m_\eta \\ 0 \end{bmatrix} \eta \tag{6.30}$$

The second and third rows of equation (6.30) may be written:

$$\begin{aligned} z_u u + z_w w + U_e q + z_\eta \eta &= 0 \\ m_u u + m_w w + m_q q + m_\eta \eta &= 0 \end{aligned} \tag{6.31}$$

Equations (6.31) may be solved algebraically to obtain expressions for w and q in terms of u and η:

$$\begin{aligned} w &= \left(\frac{m_u U_e - m_q z_u}{m_q z_w - m_w U_e}\right) u + \left(\frac{m_\eta U_e - m_q z_\eta}{m_q z_w - m_w U_e}\right) \eta \\ q &= \left(\frac{m_w z_u - m_u z_w}{m_q z_w - m_w U_e}\right) u + \left(\frac{m_w z_\eta - m_\eta z_w}{m_q z_w - m_w U_e}\right) \eta \end{aligned} \tag{6.32}$$

The expressions for w and q are substituted into rows one and four of equation (6.30) and following some rearrangement the reduced order state equation is obtained:

$$\begin{bmatrix} \dot{u} \\ \dot{\theta} \end{bmatrix} = \left[\begin{array}{c|c} x_u - x_w\left(\dfrac{m_u U_e - m_q z_u}{m_w U_e - m_q z_w}\right) & -g \\ \hline \left(\dfrac{m_u z_w - m_w z_u}{m_w U_e - m_q z_w}\right) & 0 \end{array}\right] \begin{bmatrix} u \\ \theta \end{bmatrix} + \begin{bmatrix} x_\eta - \left(\dfrac{m_\eta U_e - m_q z_\eta}{m_w U_e - m_q z_w}\right) \\ \left(\dfrac{m_\eta z_w - m_w z_\eta}{m_w U_e - m_q z_w}\right) \end{bmatrix} \eta \tag{6.33}$$

or

$$\dot{\mathbf{x}} = \mathbf{A}_p \mathbf{x} + \mathbf{B}_p \mathbf{u} \tag{6.34}$$

Equation (6.33) may be solved algebraically to obtain the response transfer functions for the phugoid variables u and θ. However, it is not very meaningful to analyse long term dynamic response to elevator in this way. The characteristic equation describing the reduced order phugoid dynamics is considerably more useful and is given by

$$\Delta(s) = \det[s\mathbf{I} - \mathbf{A}_p] = 0$$

whence

$$\begin{aligned}\Delta(s) &= s^2 + 2\zeta_p\omega_p s + \omega_p^2 \\ &= s^2 - \left(x_u - x_w\left(\frac{m_u U_e - m_q z_u}{m_w U_e - m_q z_w}\right)\right)s + g\left(\frac{m_u z_w - m_w z_u}{m_w U_e - m_q z_w}\right)\end{aligned} \tag{6.35}$$

Thus the approximate damping and natural frequency of the phugoid mode are given in terms of a limited number of aerodynamic derivatives. More explicit, but rather more approximate, insight into the aerodynamic properties of the aeroplane dominating the mode characteristics may be obtained by making some further assumptions. Typically, for conventional aeroplanes in subsonic flight:

$$m_u \to 0, \quad |m_u z_w| \ll |m_w z_u| \quad \text{and} \quad |m_w U_e| \gg |m_q z_w|$$

then the corresponding expressions for the damping and natural frequency become:

$$\begin{aligned}2\zeta_p\omega_p &= -x_u \\ \omega_p &= \sqrt{\frac{-gz_u}{U_e}}\end{aligned} \tag{6.36}$$

Now, with reference to Appendix 2:

$$x_u \cong \frac{\overset{\circ}{X}_u}{m} = \frac{\rho V_0 S X_u}{2m} \quad \text{and} \quad z_u \cong \frac{\overset{\circ}{Z}_u}{m} = \frac{\rho V_0 S Z_u}{2m} \tag{6.37}$$

since $\overset{\circ}{X}_{\dot{w}}$ is negligibly small and $m \gg \overset{\circ}{Z}_{\dot{w}}$. Expressions for the dimensionless aerodynamic derivatives are given in Appendix 8 and may be approximated as shown in expressions (6.38) when the basic aerodynamic properties are assumed to be independent of speed. This follows from the assumption that the prevailing flight condition is subsonic such that the aerodynamic properties of the airframe are not influenced by compressibility effects:

$$\begin{aligned}X_u &= -2C_D - V_0\frac{\partial C_D}{\partial V} + \left(\frac{1}{\frac{1}{2}\rho V_0 S}\right)\frac{\partial \tau}{\partial V} \cong -2C_D \\ Z_u &= -2C_L - V_0\frac{\partial C_L}{\partial V} \cong -2C_L\end{aligned} \tag{6.38}$$

Expressions (6.36) may therefore be restated in terms of aerodynamic parameters, assuming again that the trimmed lift is equal to the aircraft weight, to obtain

$$\zeta_p \omega_p = \frac{gC_D}{C_L V_0}$$

$$\omega_p = \sqrt{\frac{2g^2}{U_e V_0}} \equiv \frac{g\sqrt{2}}{V_0} \tag{6.39}$$

and a simplified approximate expression for the damping ratio follows:

$$\zeta_p \cong \frac{1}{\sqrt{2}} \left(\frac{C_D}{C_L} \right) \tag{6.40}$$

These expressions for damping ratio and natural frequency of the phugoid mode are obviously very approximate since they are the result of many simplifying assumptions. Note that the expression for ω_p is the same as that derived by Lanchester, equation (6.29), which indicates that the natural frequency of the phugoid mode is approximately inversely proportional to the trimmed speed. It is also interesting and important to note that the damping ratio of the phugoid mode is approximately inversely proportional to the *lift to drag ratio* of the aeroplane, equation (6.40). Since one of the main objectives of aeroplane design is to achieve a high lift to drag ratio it is easy to see why the damping of the phugoid mode is usually very low.

Example 6.2

To illustrate the use of reduced order models consider the A-7A Corsair II aircraft of Example 6.1 and at the same flight condition. Now the equations of motion in Example 6.1 are referred to a body axis system and the use of the reduced order models described above requires the equations of motion referred to a wind, or stability axis system. Thus, using the axis transformation relationships given in Appendices 7 and 8 the stability and control derivatives and inertia parameters referred to wind axes were calculated from the original values, which are of course referred to body axes. The longitudinal state equation was then recalculated to give

$$\begin{bmatrix} \dot{u} \\ \dot{w} \\ \dot{q} \\ \dot{\theta} \end{bmatrix} = \begin{bmatrix} -0.04225 & -0.11421 & 0 & -32.2 \\ -0.20455 & -0.49774 & 317.48 & 0 \\ 0.00003 & -0.00790 & -0.39499 & 0 \\ 0 & 0 & 1 & 0 \end{bmatrix} \begin{bmatrix} u \\ w \\ q \\ \theta \end{bmatrix} + \begin{bmatrix} 0.00381 \\ -24.4568 \\ -4.51576 \\ 0 \end{bmatrix} \eta$$

The reduced order model corresponding to the short period approximation, as given by equation (6.15), is simply taken out of equation (6.41) and is written:

$$\begin{bmatrix} \dot{w} \\ \dot{q} \end{bmatrix} = \begin{bmatrix} -0.49774 & 317.48 \\ -0.00790 & -0.39499 \end{bmatrix} \begin{bmatrix} w \\ q \end{bmatrix} + \begin{bmatrix} -24.4568 \\ -4.51576 \end{bmatrix} \eta \tag{6.41}$$

Solution of the equations of motion 6.42 using *Program CC* determines the following reduced order response transfer functions:

$$\begin{aligned}
\frac{w(s)}{\eta(s)} &= \frac{-24.457(s+59.015)}{(s^2+0.893s+2.704)} \text{ ft/s/rad} \\
\frac{q(s)}{\eta(s)} &= \frac{-4.516(s+0.455)}{(s^2+0.893s+2.704)} \text{ rad/s/rad (deg/s/deg)} \\
\frac{\alpha(s)}{\eta(s)} &= \frac{-0.077(s+59.015)}{(s^2+0.893s+2.704)} \text{ rad/rad (deg/deg)}
\end{aligned} \tag{6.42}$$

It is important to remember that these transfer functions describe, approximately, the short term response of those variables that are dominant in short period motion. The corresponding short term pitch attitude response transfer function follows since, for small perturbation motion:

$$\frac{\theta(s)}{\eta(s)} = \frac{1}{s}\frac{q(s)}{\eta(s)} = \frac{-4.516(s+0.455)}{s(s^2+0.893s+2.704)} \text{ rad/rad (deg/deg)} \tag{6.43}$$

From the pitch rate response transfer function in equations (6.43) it is readily determined that the steady state pitch rate following a positive unit step elevator input is −0.76 rad/s, which implies that the aircraft pitches continuously until the input is removed. The pitch attitude response transfer function confirms this since, after the short period transient has damped out, the aircraft behaves like a perfect integrator in pitch. This is indicated by the presence of the s term in the denominator of equation (6.44). In reality the phugoid dynamics usually prevent this situation developing unless the input is very large and accompanied by a thrust increase that results in a vertical loop manoeuvre. The model described here would be most inappropriate for the analysis of such large amplitude motion.

The common denominator of transfer functions (6.43) represents the approximate reduced order short period characteristic polynomial, equation (6.19). Thus, approximate values of the damping ratio and undamped natural frequency of the short period mode are easily calculated and are

Damping ratio $\zeta_s = 0.27$
Undamped natural frequency $\omega_s = 1.64$ rad/s

It will be seen that these values compare very favourably with the exact values given in Example 6.1.

Interpretation of the reduced order model is probably best illustrated by observing short term response to an elevator input. The responses to a 1° elevator step input of the variables given in equations (6.43) are shown in Fig. 6.5. Also shown on the same plots are the corresponding responses of the full aircraft model derived from equation (6.41). It is clear that the responses diverge with time, as expected, as no phugoid dynamics are present in the reduced order model. However, for the first ten seconds or so, the comparison is favourable indicating that the reduced order model is acceptable for most short term response studies.

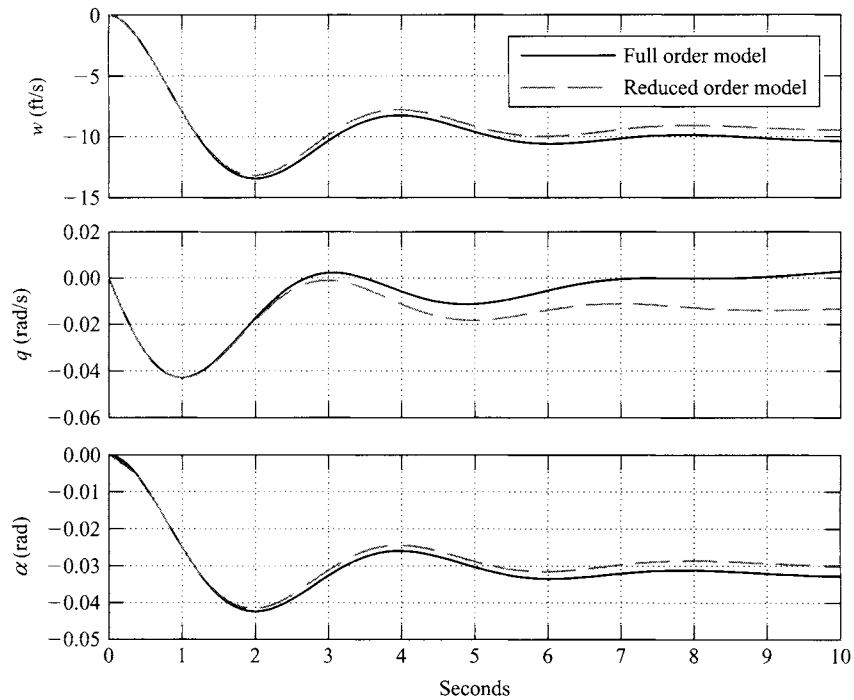

Figure 6.5 *Reduced order longitudinal response to 1° elevator step input.*

Turning now to the approximate reduced order phugoid mode characteristics. From the state equation referred to wind axes, equation (6.41), the required numerical parameters are

$$x_u = -0.04225 \text{ 1/s}$$
$$z_u = -0.20455 \text{ 1/s}$$
$$m_u = 0.00003 \text{ rad/ft/s}$$
$$U_e \equiv V_0 = 317.48 \text{ ft/s}$$

The simple Lanchester model determines that the damping of the phugoid is zero and that the undamped natural frequency is given by equation (6.29). Thus the approximate characteristics of the phugoid mode calculated according to this model are

Damping ratio $\zeta_p = 0$
Undamped natural frequency $\omega_p = 0.143$ rad/s

The approximate phugoid mode characteristics determined according to the rather more detailed reduced order model are given by equation (6.36). Since the chosen flight condition is genuinely subsonic, the derivative m_u is very small indeed which matches the constraints of the model well. The approximate characteristics of the phugoid mode calculated according to this model are

Damping ratio $\zeta_p = 0.147$
Undamped natural frequency $\omega_p = 0.144$ rad/s

Again, comparing these approximate values of the phugoid mode characteristics with the exact values in Example 6.1 indicates good agreement, especially for the undamped natural frequency. Since the phugoid damping ratio is always small (near to zero) it is very sensitive to computational rounding errors and to the approximating assumptions that make a really good approximate match difficult to achieve. The goodness of the match here is enhanced by the very subsonic flight condition that correlates well with assumptions made in the derivation of the approximate models.

6.4 FREQUENCY RESPONSE

For the vast majority of flight dynamics investigations time domain analysis is usually adequate, especially when the subject is the classical unaugmented aeroplane. The principal graphical tool used in time domain analysis is, of course, the time history plot showing the response of the aeroplane to controls or to some external disturbance. However, when the subject aeroplane is an advanced modern aeroplane fitted with a flight control system, flight dynamics analysis in the frequency domain can provide additional valuable insight into its behaviour. In recent years frequency domain analysis has made an important contribution to the understanding of the sometimes unconventional handling qualities of aeroplanes whose flying qualities are largely shaped by a flight control system. It is for this reason that a brief review of simple frequency response ideas is considered here. Since frequency response analysis tools are fundamental to classical control engineering their description can be found in almost every book on the subject; very accessible material can be found in Shinners (1980) and Friedland (1987) for example.

Consider the hypothetical situation when the elevator of an otherwise trimmed aeroplane is operated sinusoidally with constant amplitude k and variable frequency ω; the longitudinal input to the aeroplane may therefore be expressed:

$$\eta(t) = k \sin \omega t \tag{6.44}$$

It is reasonable to expect that each of the output variables describing aircraft motion will respond sinusoidally to the input. However, the amplitudes of the output variables will not necessarily be the same and they will not necessarily be in phase with one another or with the input. Thus the general expression describing any output response variable may be written:

$$y(t) = K \sin(\omega t + \phi) \tag{6.45}$$

where both the output amplitude K and phase shift ϕ are functions of the exciting frequency ω. As the exciting frequency ω is increased from zero so, initially, at low frequencies, the sinusoidal response will be clearly visible in all output variables. As the exciting frequency is increased further so the sinusoidal response will start to diminish in magnitude and will eventually become imperceptible in the outputs. Simultaneously, the phase shift ϕ will indicate an increasingly large lag between the input and output. The reason for these observations is that at sufficiently high frequencies the mass and inertia properties of the aeroplane simply prevent it responding quickly enough to follow the input. The limiting frequency at which the response commences

to diminish rapidly is referred to as the *bandwidth* of the aeroplane with respect to the output variable of interest. A more precise definition of bandwidth is given below. Since aeroplanes only respond to frequencies below the bandwidth frequency they have the frequency response properties of a *low pass system*. At exciting frequencies corresponding to the damped natural frequencies of the phugoid and the short period mode, peaks in output magnitude K will be seen together with significant changes in phase shift ϕ. The mode frequencies are described as *resonant frequencies* and the magnitudes of the output parameters K and ϕ at *resonance* are determined by the damping ratios of the modes. The system (or aeroplane) *gain* in any particular response variable is defined:

$$\text{System gain} = \left| \frac{K(\omega)}{k} \right| \tag{6.46}$$

where, in normal control system applications, it is usually assumed that the input and output variables have the same units. This is often not the case in aircraft applications and care must be exercised in the interpretation of gain.

A number of graphical tools have been developed for the frequency response analysis of linear systems and include the Nyquist diagram, the Nichols chart and the Bode diagram. All are intended to simplify analytical procedures, the mathematical calculation of which is tedious without a computer, and all plot input–output gain and phase as functions of frequency. Perhaps the simplest of the graphical tools to use and interpret is the Bode diagram although the amount of information it is capable of providing is limited. However, today it is used extensively for flight dynamics analysis, especially in advanced handling qualities studies.

6.4.1 The Bode diagram

The intention here is not to describe the method for constructing a Bode diagram but to describe its application to the aeroplane and to explain its correct interpretation. For an explanation of the method for constructing a Bode diagram the reader should consult a suitable control engineering text, such as either of those referenced above.

To illustrate the application of the Bode diagram to a typical classical aeroplane consider the pitch attitude response to elevator transfer function as given by equation (6.5):

$$\frac{\theta(s)}{\eta(s)} = \frac{k_\theta(s + (1/T_{\theta_1}))(s + (1/T_{\theta_2}))}{(s^2 + 2\zeta_p\omega_p s + \omega_p^2)(s^2 + 2\zeta_s\omega_s s + \omega_s^2)} \tag{6.47}$$

This response transfer function is of particular relevance to longitudinal handling studies and it has the simplifying advantage that both the input and output variables have the same units. Typically, in frequency response calculation it is usual to assume a sinusoidal input signal of unit magnitude. It is also important to note that whenever the response transfer function is negative, which is often the case in aircraft applications, a negative input is assumed that ensures the correct computation of phase. Therefore, in this particular application, since k_θ is usually a negative number a sinusoidal elevator input of unit magnitude, $\eta(t) = -1 \sin \omega t$ is assumed. The pitch attitude frequency

response is calculated by writing $s = j\omega$ in equation (6.48); the right hand side then becomes a complex number whose magnitude and phase can be evaluated for a suitable range of frequency ω. Since the input magnitude is unity the *system gain*, equation (6.47), is given simply by the absolute value of the magnitude of the complex number representing the right hand side of equation (6.48) and is, of course, a function of frequency ω.

Since the calculation of gain and phase involves the products of several complex numbers it is preferred to work in terms of the logarithm of the complex number representing the transfer function. The total gain and phase then become the simple sums of the gain and phase of each factor in the transfer function. For example, each factor in parentheses on the right hand side of equation (6.48) may have its gain and phase characteristics calculated separately as a function of frequency; the total gain and phase is then given by summing the contributions from each factor. However, the system gain is now expressed as a logarithmic function of the gain ratio, equation (6.47), and is defined:

$$\text{Logarithmic gain} = 20 \log_{10} \left| \frac{K(\omega)}{k} \right| \text{dB} \tag{6.48}$$

and has units of *decibels* denoted dB. Fortunately it is no longer necessary to calculate frequency response by hand since many computer software packages, such as *MATLAB*, have this facility and can also provide the desired graphical output. However, as always, some knowledge of the analytical procedure for obtaining frequency response is essential so that the computer output may be correctly interpreted.

The Bode diagram comprises two corresponding plots, the *gain plot* and the *phase plot*. The gain plot shows the logarithmic gain, in dB, plotted against $\log_{10}(\omega)$ and the phase plot shows the phase, in degrees, also plotted against $\log_{10}(\omega)$. To facilitate interpretation the two plots are often superimposed on a common frequency axis. The Bode diagram showing the typical pitch attitude frequency response, as given by transfer function (6.48), is shown in Fig. 6.6.

Also shown in Fig. 6.6 are the asymptotic approximations to the actual gain and phase plots as functions of frequency. The asymptotes can be drawn in simply from inspection of the transfer function, equation (6.48), and serve as an aid to interpretation. Quite often the asymptotic approximation is sufficient for the evaluation in hand, thereby dispensing with the need to compute the actual frequency response entirely.

The shape of the gain plot is characterised by the *break frequencies* $\omega 1$ to $\omega 4$ which determine the locations of the discontinuities in the asymptotic gain plot. Each break frequency is defined by a key frequency parameter in the transfer function, namely

$$\omega 1 = \frac{1}{T_{\theta_1}} \quad \text{with first order phase lead } (+45°)$$

$$\omega 2 = \omega_p \quad \text{with second order phase lag } (-90°)$$

$$\omega 3 = \frac{1}{T_{\theta_2}} \quad \text{with first order phase lead } (+45°)$$

$$\omega 4 = \omega_s \quad \text{with second order phase lag } (-90°)$$

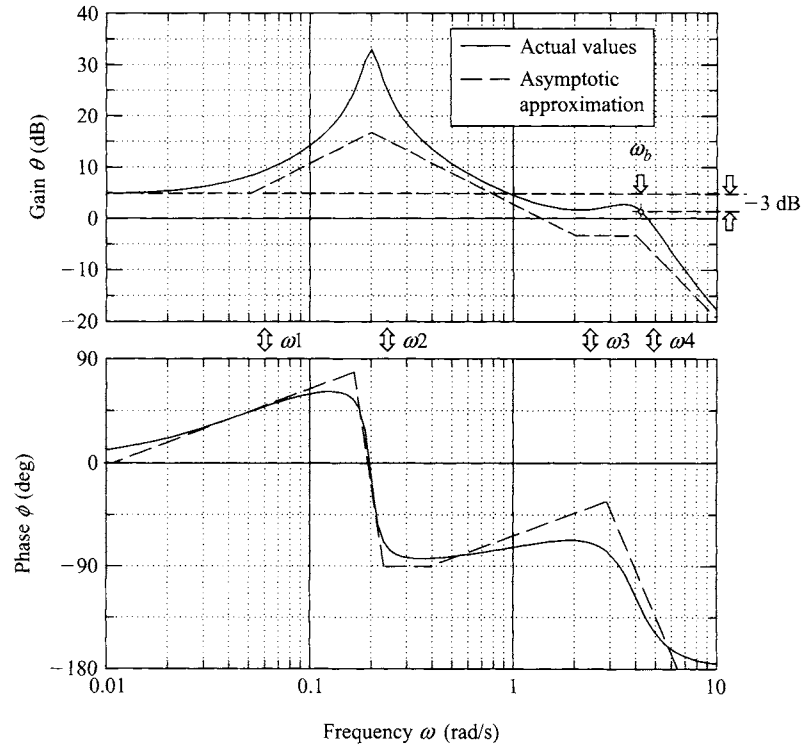

Figure 6.6 *Bode diagram showing classical pitch attitude frequency response.*

Since the transfer function is classical minimum phase, the corresponding phase shift at each break frequency is a *lead* if it arises from a numerator term or a *lag* if it arises from a denominator term. If, as is often the case in aircraft studies, non-minimum phase terms appear in the transfer function then, their frequency response properties are unchanged except that the sign of the phase is reversed. Further, a first order term gives rise to a total phase shift of 90° and a second order term gives rise to a total phase shift of 180°. The characteristic phase response is such that half the total phase shift associated with any particular transfer function factor occurs at the corresponding break frequency. Armed with this limited information a modest interpretation of the pitch attitude frequency response of the aeroplane is possible. The frequency response of the other motion variables may be dealt with in a similar way.

6.4.2 Interpretation of the Bode diagram

With reference to Fig. 6.6 it is seen that at very low frequencies, $\omega < 0.01$ rad/s, there is no phase shift between the input and output and the gain remains constant, at a little below 5 dB in this illustration. In other words, the pitch attitude will follow the stick movement more or less precisely. As the input frequency is increased through $\omega 1$ so the pitch response leads the input in phase, the output magnitude increases rapidly and

the aeroplane appears to behave like an *amplifier*. At the phugoid frequency the output reaches a substantial peak, consistent with the low damping, and thereafter the gain drops rapidly accompanied by a rapid increase in phase lag. As the input frequency is increased further so the gain continues to reduce gently and the phase settles at $-90°$ until the influence of break frequency $\omega 3$ comes into play. The reduction in gain is arrested and the effect of the phase lead may be seen clearly. However, when the input frequency reaches the short period break frequency a small peak in gain is seen, consistent with the higher damping ratio, and at higher frequencies the gain continues to reduce steadily. Meanwhile, the phase lag associated with the short period mode results in a constant total phase lag of $-180°$ at higher frequencies.

Once the output–input gain ratio drops below unity, or 0 dB, the aeroplane appears to behave like an *attenuator*. The frequency at which the gain becomes sufficiently small that the magnitude of the output response becomes insignificant is called the *bandwidth frequency*, denoted ω_b. There are various definitions of bandwidth, but the definition used here is probably the most common and defines the bandwidth frequency as the frequency at which the gain first drops to -3 dB below the zero frequency, or steady state, gain. The bandwidth frequency is indicated in Fig. 6.6 and it is commonly a little higher than the short period frequency. A gain of -3 dB corresponds with a gain ratio of $1/\sqrt{2} = 0.707$. Thus, by definition, the gain at the bandwidth frequency is 0.707 times the steady state gain. Since the pitch attitude bandwidth frequency is close to the short period frequency the latter may sometimes be substituted for the bandwidth frequency which is often good enough for most practical purposes.

The peaks in the gain plot are determined by the characteristics of the stability modes. A very pronounced peak indicates low mode damping and *vice versa*; an infinite peak corresponding with zero damping. The magnitude of the changes in gain and phase occurring in the vicinity of a peak indicates the significance of the mode in the response variable in question. Figure 6.6 indicates the magnitude of the phugoid to be much greater than the magnitude of the short period mode in the pitch response of the aeroplane. This would, in fact, be confirmed by response time histories and inspection of the corresponding eigenvectors.

In the classical application of the Bode diagram, as used by the control engineer, inspection of the gain and phase properties in the vicinity of the bandwidth frequency enables conclusions about the stability of the system to be made. Typically, stability is quantified in terms of *gain margin* and *phase margin*. However, such evaluations are only appropriate when the system transfer function is *minimum phase*. Since aircraft transfer functions that are non-minimum phase are frequently encountered, and many also have the added complication that they are negative, it is not usual for aircraft stability to be assessed on the Bode diagram. It is worth noting that, for aircraft augmented with flight control systems, the behaviour of the phase plot in the vicinity of the bandwidth frequency is now known to be linked to the susceptibility of the aircraft to *pilot induced oscillations*, a particularly nasty handling deficiency.

Now the foregoing summary interpretation of frequency response assumes a sinusoidal elevator input to the aircraft. Clearly, this is never likely to occur as a result of normal pilot action. However, normal pilot actions may be interpreted to comprise a mix of many different frequency components. For example, in gentle manoeuvring the frequency content of the input would generally be low whilst, in aggressive or high

workload situations the frequency content would be higher and might even exceed the bandwidth of the aeroplane. In such a limiting condition the pilot would certainly be aware that the aeroplane could not follow his demands quickly enough and, depending in detail on the gain and phase response properties of the aeroplane, he could well encounter hazardous handling problems. Thus bandwidth is a measure of the *quickness of response* achievable in a given aeroplane. As a general rule it is desirable that flight control system designers should seek the highest response bandwidth consistent with the dynamic capabilities of the airframe.

Example 6.3

The longitudinal frequency response of the A-7A Corsair II aircraft is evaluated for the same flight condition as Examples 6.1 and 6.2. However, the longitudinal response transfer functions used for the evaluations are referred to wind axes and were obtained in the solution of the full order state equation (6.41). The transfer functions of primary interest are

$$\begin{aligned}
\frac{u(s)}{\eta(s)} &= \frac{0.00381(s+0.214)(s+135.93)(s+598.3)}{(s^2+0.033s+0.02)(s^2+0.902s+2.666)} \text{ ft/s/rad} \\
\frac{\theta(s)}{\eta(s)} &= \frac{-4.516(s-0.008)(s+0.506)}{(s^2+0.033s+0.02)(s^2+0.902s+2.666)} \text{ rad/rad} \\
\frac{\alpha(s)}{\eta(s)} &= \frac{-0.077(s^2+0.042s+0.02)(s+59.016)}{(s^2+0.033s+0.02)(s^2+0.902s+2.666)} \text{ rad/rad}
\end{aligned} \tag{6.49}$$

It will be noticed that the values of the various numerator terms in the velocity and incidence transfer functions differ significantly from the values in the corresponding transfer functions in Example 6.1, equation (6.8). This is due to the different reference axes used and to the fact that the angular difference between body and wind axes is a significant body incidence angle of 13.3°. Such a large angle is consistent with the very low speed flight condition. The frequency response of each transfer function was calculated with the aid of *Program CC* and the Bode diagrams are shown in Figures 6.7–6.9 respectively. Interpretation of the Bode diagrams for the three variables is straightforward and follows the general interpretation discussed above. However, important or significant differences are commented on as follows.

The frequency response of axial velocity u to elevator input η is shown in Fig. 6.7 and it is clear, as might be expected, that it is dominated by the phugoid. The very large low frequency gain values are due entirely to the transfer function units that are ft/s/rad, and a unit radian elevator input is of course unrealistically large! The peak gain of 75 dB at the phugoid frequency corresponds with a gain ratio of approximately 5600 ft/s/rad. However, since the aircraft model is linear, this very large gain ratio may be interpreted equivalently as approximately 98 ft/s/deg, which is much easier to appreciate physically. Since the gain drops away rapidly as the frequency increases beyond the phugoid frequency, the velocity bandwidth frequency is only a little higher than the phugoid frequency. This accords well with practical observation; velocity

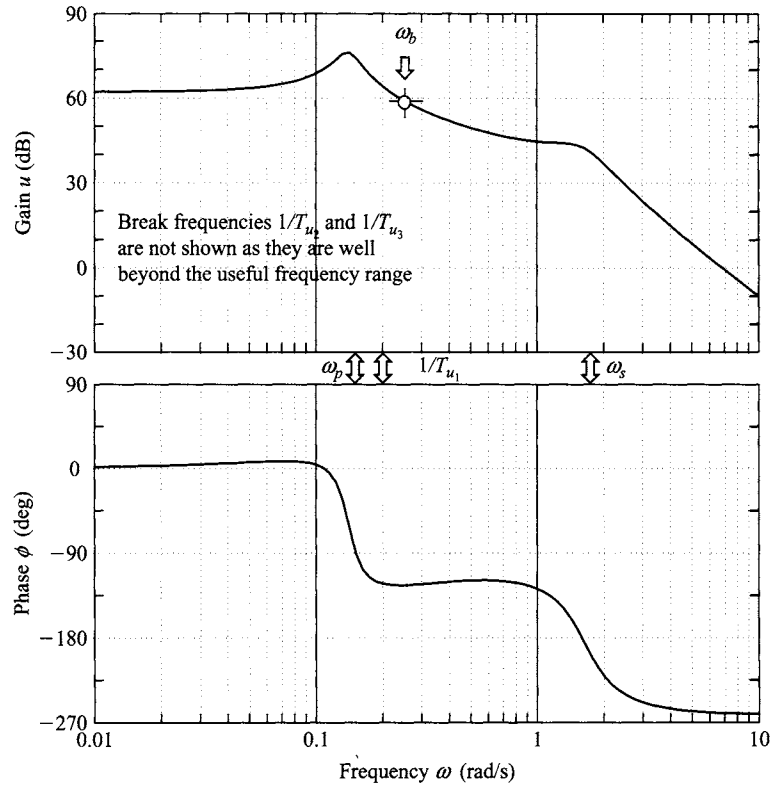

Figure 6.7 *A-7A velocity frequency response.*

perturbations at frequencies in the vicinity of the short period mode are usually insignificantly small. The phase plot indicates that there is no appreciable phase shift between input and output until the frequency exceeds the phugoid frequency when there is a rapid increase in phase lag. This means that for all practical purposes speed changes demanded by the pilot will follow the stick in the usable frequency band.

The pitch attitude θ frequency response to elevator input η is shown in Fig. 6.8. Its general interpretation follows the discussion of Fig. 6.6 and is not repeated here. However, there are some significant differences which must not be overlooked. The differences are due to the fact that the transfer function is non-minimum phase, a consequence of selecting a very low speed flight condition for the example. Referring to equations (6.50), this means that the numerator zero $1/T_{\theta_1}$ is negative, and the reasons for this are discussed in Example 6.1. The non-minimum phase effects do not influence the gain plot in any significant way, so its interpretation is quite straightforward. However, the effect of the non-minimum phase numerator zero is to introduce phase lag at very low frequencies rather than the usual phase lead. It is likely that in manoeuvring at this flight condition the pilot would be aware of the pitch attitude lag in response to his stick input.

The body incidence α frequency response to elevator input η is shown in Fig. 6.9 and it is clear that, as might be expected, this is dominated by the short period

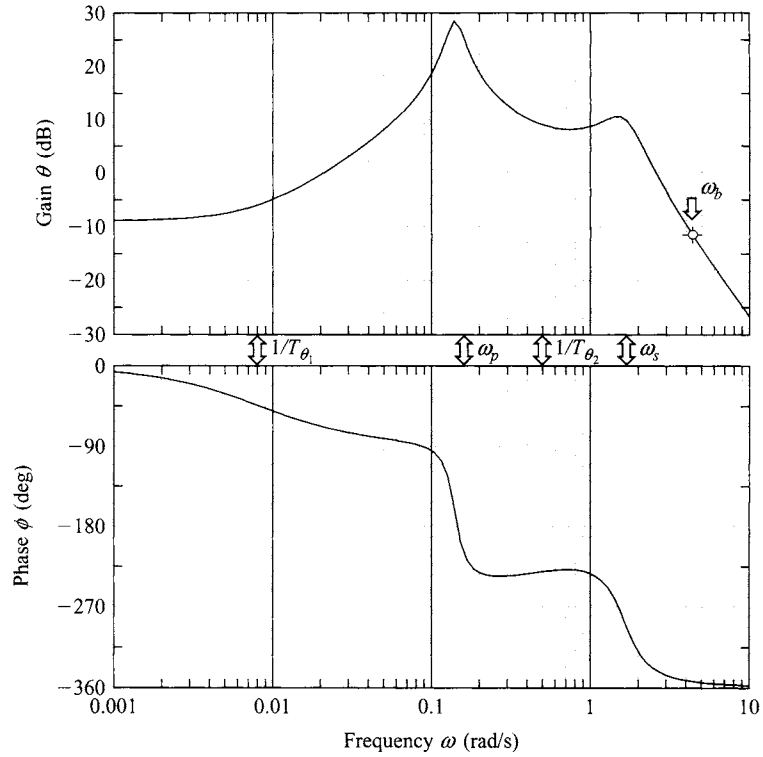

Figure 6.8 *A-7A pitch attitude frequency response.*

mode. For all practical purposes the influence of the phugoid on both the gain and phase frequency responses is insignificant. This may be confirmed by reference to the appropriate transfer function in equations (6.50), where it will be seen that the second order numerator term very nearly cancels the phugoid term in the denominator. This is an important observation since it is quite usual to cancel approximately equal numerator and denominator terms in any response transfer function to simplify it. Simplified transfer functions often provide adequate response models in both the time and frequency domains, and can be extremely useful for explaining and interpreting aircraft dynamic behaviour. In modern control parlance the phugoid dynamics would be said to be *not observable* in this illustration. The frequency response in both gain and phase is more or less *flat* at frequencies up to the short period frequency, or for most of the usable frequency range. In practical terms this means that incidence will follow the stick at constant gain and without appreciable phase lag, which is obviously a desirable state of affairs.

6.5 FLYING AND HANDLING QUALITIES

The longitudinal stability modes play an absolutely fundamental part in determining the longitudinal flying and handling qualities of an aircraft and it is essential that their

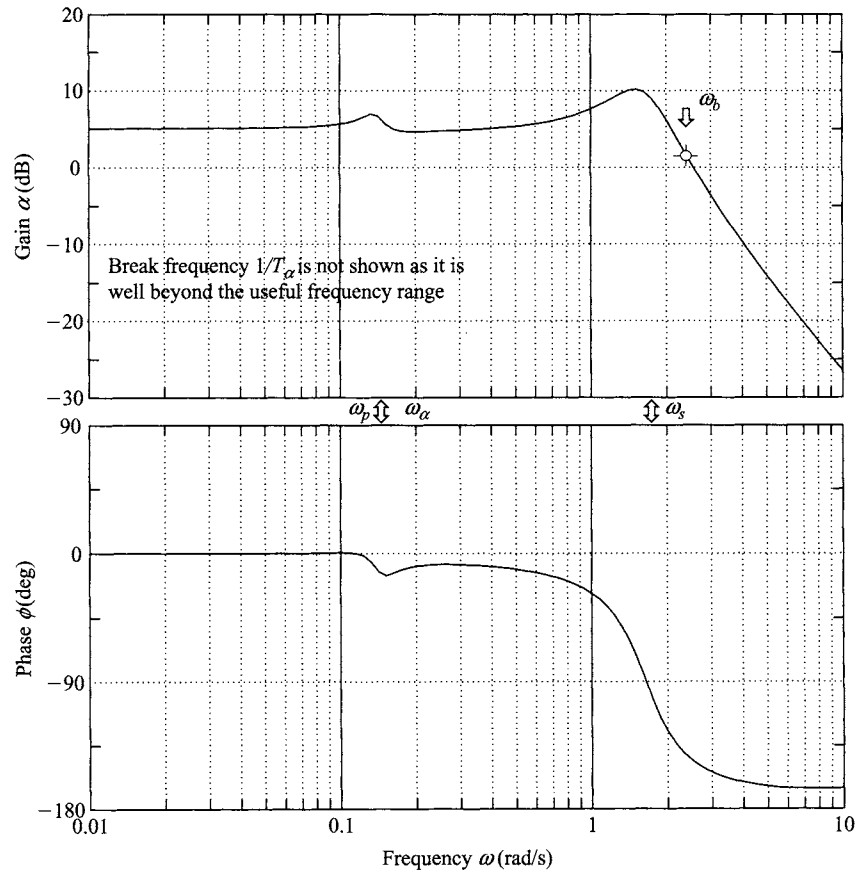

Figure 6.9 *A-7A body incidence frequency response.*

characteristics must be "correct" if the aircraft is to be flown by a human pilot. A simplistic view of the human pilot suggests that he behaves like an adaptive dynamic system and will adapt his dynamics to harmonise with those of the controlled vehicle. Since his dynamics interact and couple with those of the aircraft he will adapt, within human limits, to produce the best *closed loop* system dynamics compatible with the piloting task. His adaptability enables him to cope well with aircraft with less than desirable flying qualities. However, the problems of coupling between incompatible dynamic systems can be disastrous and it is this latter aspect of the piloting task that has attracted much attention in recent years. Every time the aircraft is disturbed in response to control commands the stability modes are excited and it is not difficult to appreciate why their characteristics are so important. Similarly, the stability modes are equally important in determining *ride quality* when the main concern is response to atmospheric disturbances. In military combat aircraft ride quality determines the effectiveness of the airframe as a weapons platform and in the civil transport aircraft it determines the comfort of passengers.

In general it is essential that the short period mode, which has a natural frequency close to human pilot natural frequency, is adequately damped. Otherwise, dynamic coupling with the pilot may occur under certain conditions leading to severe, or even catastrophic, handling problems. On the other hand, as the phugoid mode is much lower in frequency its impact on the piloting task is much less demanding. The average human pilot can easily control the aircraft even when the phugoid is mildly unstable. The phugoid mode can, typically, manifest itself as a minor trimming problem when poorly damped. Although not in itself hazardous, it can lead to increased pilot workload and for this reason it is desirable to ensure adequate phugoid damping. It is also important that the natural frequencies of the stability modes should be well separated in order to avoid interaction, or coupling, between the modes. Mode coupling may give rise to unusual handling characteristics and is generally regarded as an undesirable feature in longitudinal dynamics. The subject of aircraft handling qualities is discussed in rather more detail in Chapter 10.

6.6 MODE EXCITATION

Since the longitudinal stability modes are usually well separated in frequency, it is possible to excite the modes more or less independently for the purposes of demonstration or measurement. Indeed, it is a general flying qualities requirement that the modes be well separated in frequency in order to avoid handling problems arising from dynamic mode coupling. The modes may be excited selectively by the application of a sympathetic elevator input to the trimmed aircraft. The methods developed for in-flight mode excitation reflect an intimate understanding of the dynamics involved and are generally easily adapted to the analytical environment. Because the longitudinal modes are usually well separated in frequency the form of the input disturbance is not, in practice, very critical. However, some consistency in the flight test or analytical procedures adopted is desirable if meaningful comparative studies are to be made.

The short period pitching oscillation may be excited by applying a short duration disturbance in pitch to the trimmed aircraft. This is best achieved with an elevator pulse having a duration of a second or less. Analytically this is adequately approximated by a unit impulse applied to the elevator. The essential feature of the disturbance is that it must be sufficiently short so as not to excite the phugoid significantly. However, as the phugoid damping is usually very low it is almost impossible not to excite the phugoid at the same time but, it does not usually develop fast enough to obscure observation of the short period mode. An example of a short period response recorded during a flight test exercise in a Handley Page Jetstream aircraft is shown in Fig. 6.10. In fact two excitations are shown, the first in the nose up sense and the second in the nose down sense. The pilot input "impulse" is clearly visible and represents his best attempt at achieving a clean impulse like input; some practice is required before consistently good results are obtained. Immediately following the input the pilot released the controls to obtain the controls free dynamic response which explains why the elevator angle does not recover its equilibrium trim value until the short period transient has settled. During this short elevator free period its motion is driven by oscillatory aerodynamic loading and is also coloured by the control circuit

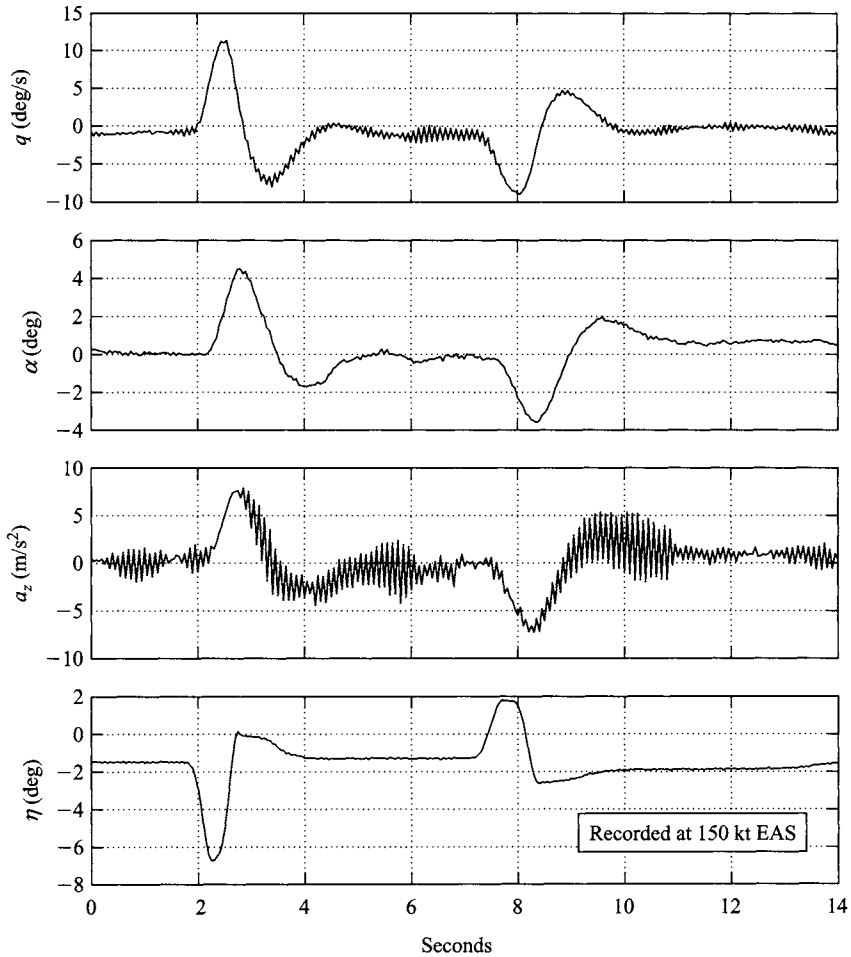

Figure 6.10 *Flight recording of the short period pitching oscillation.*

dynamics which can be noticeably intrusive. Otherwise the response is typical of a well damped aeroplane.

The phugoid mode may be excited by applying a small speed disturbance to the aircraft in trimmed flight. This is best achieved by applying a small step input to the elevator which will cause the aircraft to fly up, or down, according to the sign of the input. If the power is left at its trimmed setting then the speed will decrease, or increase, accordingly. When the speed has diverged from its steady trimmed value by about 5% or so, the elevator is returned to its trim setting. This provides the disturbance and a stable aircraft will then execute a phugoid oscillation as it recovers its trim equilibrium. Analytically, the input is equivalent to an elevator pulse of several seconds duration. The magnitude and length of the pulse would normally be established by trial and error since its effect will be very aircraft dependent. However, it should be remembered that for proper interpretation of the resulting response the

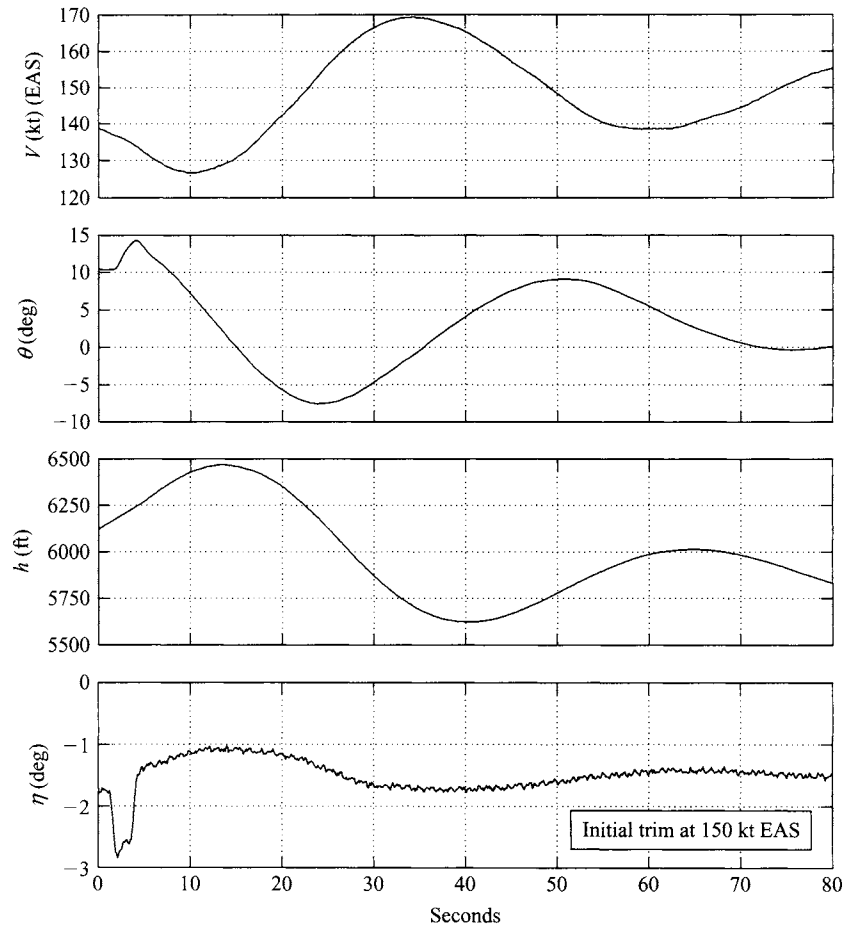

Figure 6.11 *Flight recording of the phugoid.*

disturbance should be small in magnitude since a small perturbation model is implied. An example of a phugoid response recorded during a flight test exercise in a Handley Page Jetstream aircraft is shown in Fig. 6.11. The pilot input "pulse" is clearly visible and, as for the short period mode, some practice is required before consistently good results are obtained. Again, the controls are released following the input to obtain the controls free dynamic response and the subsequent elevator motion is caused by the sinusoidal aerodynamic loading on the surface itself. The leading and trailing edge steps of the input elevator pulse may excite the short period mode. However, the short period mode transient would normally decay to zero well before the phugoid has properly developed and would not therefore obscure the observation of interest.

It is clear from an inspection of Fig. 6.11 that the phugoid damping is significantly higher than might be expected from the previous discussion of the mode characteristics. What is in fact shown is the aerodynamic, or basic airframe, phugoid modified by

the inseparable effects of power. The Astazou engines of the Jetstream are governed to run at constant rpm and thrust changes are achieved by varying the propeller blade pitch. Thus as the aircraft flies the sinusoidal flight path during a phugoid disturbance the sinusoidal propeller loading causes the engine to automatically adjust its power to maintain constant propeller rpm. This very effectively increases the apparent damping of the phugoid. It is possible to operate the aircraft at a constant power condition when the "power damping" effect is suppressed. Under these circumstances it is found that the aerodynamic phugoid is much less stable, as predicted by the simple theoretical model, and at some flight conditions it is unstable.

The above flight recording of the longitudinal stability modes illustrates the *controls free* dynamic stability characteristics. The same exercise could of course be repeated with the controls held fixed following the disturbing input. In this event the *controls fixed* dynamic stability characteristics would be observed. In general the differences between the responses would be small and not too significant. Now controls free dynamic response is only possible in aeroplanes with reversible controls which includes most small classical aeroplanes. Virtually all larger modern aircraft have powered controls, driven by electronic flight control systems, which are effectively irreversible and which means that they are only capable of exhibiting controls fixed dynamic response. Thus, today, most theoretical modelling and analysis is concerned with controls fixed dynamics only, as is the case throughout this book. However, a discussion of the differences between controls fixed and controls free aeroplane dynamics may be found in Hancock (1995).

When it is required to analyse the dynamics of a single mode in isolation, the best approach is to emulate flight test practice as far as that is possible. It is necessary to choose the most appropriate transfer functions to show the dominant response variables in the mode of interest. For example, as shown in Figures 6.10 and 6.11 the short period mode is best observed in the dominant response variables q and $w(\alpha)$ whereas the phugoid is best observed in its dominant response variables u, h and θ. It is necessary to apply a control input disturbance sympathetic to the mode dynamics and it is necessary to observe the response for an appropriate period of time. For example, Fig. 6.1 shows both longitudinal modes but the time scale of the illustration reveals the phugoid in much greater detail than the short period mode, whereas the time scale of Fig. 6.5 was chosen to reveal the short period mode in detail since that is the mode of interest. The form of the control input is not usually difficult to arrange in analytical work since most software packages have built-in impulse, step and pulse functions, whilst more esoteric functions can usually be programmed by the user. This kind of informed approach to the analysis is required if the best possible visualisation of the longitudinal modes and their associated dynamics is to be obtained.

REFERENCES

Friedland, B. 1987: *Control System Design.* McGraw-Hill Book Company, New York.

Hancock, G.J. 1995: *An Introduction to the Flight Dynamics of Rigid Aeroplanes.* Ellis Horwood Ltd., Hemel Hempstead.

Lanchester, F.W. 1908: *Aerodonetics.* Macmillan and Co.

Shinners, S.M. 1980: *Modern Control System Theory and Application.* Addison-Wesley Publishing Co, Reading, Massachusetts.

Teper, G.L. 1969: *Aircraft Stability and Control Data.* Systems Technology, Inc., STI Technical Report 176-1. NASA Contractor Report, National Aeronautics and Space Administration, Washington D.C. 20546.

PROBLEMS

1. A tailless aeroplane of 9072 kg mass has an aspect ratio 1 delta wing of area 37 m^2. The longitudinal short period motion of the aeroplane is described by the characteristic quadratic:

$$\lambda^2 + B\lambda + C = 0 \quad \text{where } B = \frac{1}{2}\left(\frac{dC_L}{d\alpha}\right)\cos^2\alpha \text{ and}$$

$$C = -\frac{1}{2}\left(\frac{\mu_1}{i_y}\right)\left(\frac{dC_m}{d\alpha}\right)\cos\alpha.$$

α is the wing incidence, $\mu_1 = m/\frac{1}{2}\rho S\bar{c}$ is the longitudinal relative density parameter, and $i_y = I_y/m\bar{c}^2$ is the dimensionless moment of inertia in pitch. The aeroplane's moment of inertia in pitch is 1.356×10^5 kg/m^2. The variation of C_L and C_m with incidence $\alpha > 0$ is non-linear for the aspect ratio 1 delta wing:

$$C_L = \frac{1}{2}\pi\alpha + 2\alpha^2$$

$$C_m = C_{m_0} - 0.025\pi\alpha - 0.1\alpha^2$$

Compare and describe the short period motions when the aeroplane is flying straight and level at 152 m/s at sea level and at 35,000 ft.

$\rho_0 = 1.225$ kg/m^3 at sea level, $\rho/\rho_0 = 0.310$ at 35,000 ft. Characteristic time $\sigma = m/\frac{1}{2}\rho V_0 S$. (CU 1983)

2. (i) List the characteristics of the longitudinal phugoid stability mode.
   (ii) List the characteristics of the longitudinal short period pitching stability mode.
   (iii) The transfer function for the unaugmented McDonnell F-4C Phantom describing the pitch attitude response to elevator when flying at Mach 1.2 at an altitude of 35,000 ft is given by

$$\frac{\theta(s)}{\eta(s)} = \frac{-20.6(s + 0.013)(s + 0.62)}{(s^2 + 0.017s + 0.002)(s^2 + 1.74s + 29.49)} \text{ rad/rad}$$

   Write down the longitudinal characteristic equation and state whether the aeroplane is stable, or not.
   (iv) What are the numerical parameters describing the longitudinal stability modes of the McDonnell F-4C Phantom? (CU 1999)
3. Describe the longitudinal short period pitching oscillation. On what parameters do its characteristics depend?

A model aircraft is mounted in a wind tunnel such that it is free to pitch about an axis through its *cg* as shown. The model is restrained by two springs attached at a point on a fuselage aft extension which is at a distance $l = 0.5$ m from the *cg*. The model has wing span $b = 0.8$ m, mean aerodynamic chord $\bar{\bar{c}} = 0.15$ m and the air density may be taken as $\rho = 1.225\,\text{kg/m}^3$.

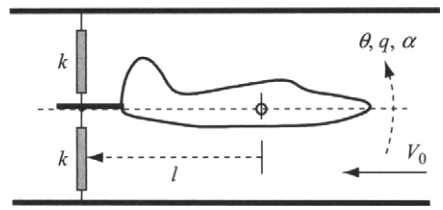

With the wind off the model is displaced in pitch and released. The frequency of the resulting oscillation is 10 rad/s and the damping ratio 0.1. The experiment is repeated with a wind velocity $V_0 = 30$ m/s, the frequency is now found to be 12 rad/s and the damping ratio 0.3. Given that the spring stiffness $k = 16$ N/m, calculate the moment of inertia in pitch, and values for the dimensionless stability derivatives M_q and M_w. It may be assumed that the influence of the derivative $M_{\dot{w}}$ is negligible. State all assumptions made. (CU 1987)

4. (i) Show that the period of the phugoid is given approximately by, $T_p = \sqrt{2}\pi \frac{V_0}{g}$, and state all assumptions used during the derivation.
   (ii) State which aerodynamic parameters introduce damping into a phugoid, and discuss how varying forward speed whilst on approach to landing may influence phugoid characteristics. (LU 2001)
5. (i) Using a simple physical model, show that the short period pitching oscillation can be approximated to by

$$I_y\ddot{\theta} + \frac{1}{2}\rho V_0 a_1 S_T l_T^2 \dot{\theta} - \frac{1}{2}\rho V_0^2 S\bar{\bar{c}}\frac{\mathrm{d}C_m}{\mathrm{d}\alpha}\theta = 0$$

   (ii) The aircraft described below is flying at sea level at 90 m/s. Determine the *cg* location at which the short period pitching oscillation ceases to be oscillatory:

Wing lift curve slope	$= 5.7$ 1/rad
Tailplane lift curve slope	$= 3.7$ 1/rad
Horizontal tail arm	$= 6$ m
Tailplane area	$= 5\,\text{m}^2$
$\mathrm{d}\varepsilon/\mathrm{d}\alpha$	$= 0.30$
I_y	$= 40{,}000\,\text{kg/m}^2$
Wing area	$= 30\,\text{m}^2$
Mean aerodynamic chord	$= 1.8$ m
Aerodynamic centre	$= 0.18\bar{\bar{c}}$

(Hint: Modify the equation in part (i) to include tailplane lag effects.)

(iii) Determine the period of the short period pitching oscillation if the *cg* location is moved $0.2\bar{c}$ forward of the position calculated in part (ii). (LU 2001)

6. For a conventional aircraft on an approach to landing, discuss how the aircraft's aerodynamics may influence longitudinal stability. (LU 2002)
7. Determine the time to half amplitude and the period of the short period pitching oscillation. Assume that the short period pitching oscillation can be approximated by

$$I_y\ddot{\theta} - \frac{\partial M}{\partial q}\dot{\theta} - \frac{\partial M}{\partial w}V\theta = 0 \quad \text{and in addition } M_w = \partial C_m/\partial\alpha. \qquad \text{(LU 2003)}$$